

Effects of Crystal Growth Conditions of n-type Cz-Si for Solar Cells on Oxygen Precipitation and Dislocation Formation through Annealing Process

Kosuke Kinoshita¹, Takuto Kojima¹, Kohei Onishi¹, Yoshio Ohshita² and Atushi Ogura¹

¹ Meiji Univ.

1-1-1 Higashimita, Tama-ku, Kawasaki, Kanagawa 214-8571, Japan

Phone: +81-44-934-7352 E-mail: ce171022@meiji.ac.jp

² Toyota Tech. Inst.

2-12-1 Hisakata, Tenpaku-ku, Nagoya, Aichi 468-8511, Japan

Abstract

In this study, the effects of oxygen precipitation and dislocation formation on the minority carrier lifetime were evaluated in conjunction with crystal growth conditions. It was revealed that oxygen precipitates and dislocations formation are controlled and lifetime deterioration is suppressed in Cz-Si which is kept at the high temperature and rapidly cooling during crystal growth. We have shown that controlling oxygen precipitation by crystal growth conditions can contribute to high efficiency of solar cells.

1. Introduction

Since n-type mono crystalline Si has longer carrier lifetime than p-type, it is expected to be applied to the next-generation solar cells [1]. Oxygen is incorporated in the Si crystal grown by the Czochralski (Cz) crystal growth. The oxygen precipitation proceeds during the annealing processes, which causes a reduction in the solar cell efficiency [2]. Therefore, it is important to understand and control the oxygen precipitation behavior to improve the solar cell performance.

In this study, wafers fabricated by different crystal growth conditions were prepared, and the effects of oxygen precipitation and dislocation formation through annealing process on the minority carrier lifetime was evaluated.

2. Experiment

In order to investigate the influence of crystal growth conditions for oxygen precipitation, two kinds of substrates fabricated by different crystal growth conditions, namely conventional (Conv.) process and advanced (Adv.) process, were prepared with the same range of oxygen concentration ($1.8\text{--}2.1 \times 10^{18} \text{ cm}^{-3}$). Conventional process is a typical Cz crystal growth, whereas advanced process keeps the high temperature by using a heater and then is rapidly cooling. These two crystal growth conditions differ only in the thermal history during crystal growth with keeping the total process time the same. Annealing process was performed at 1100°C for 3, 6 and 9 h, respectively. After the both surfaces of the sample were mirror polished, the precipitate density and diameter were measured by infrared light scattering tomography (IR-LST). The photo-luminescence (PL) intensity was measured as an index of the minority carrier lifetime. A bandpass filter ($1140 \pm 90 \text{ nm}$), an InGaAs imager as the detector, and a near-infrared laser with an excitation wavelength of 808 nm were

used. The penetration depth of the laser is approximately $10 \mu\text{m}$, and the bulk band-edge emission was measured. Thereafter, Sopori etching was applied to the sample after 1100°C for 9 h annealing, then the etch pits were observed with the optical microscope, to evaluate dislocations [3-5].

3. Results and Discussion

Figure 1 shows the correlation between carbon concentration and PL intensity depending on crystal growth conditions. In both processes, the minority carrier lifetime decreased as the carbon concentration increased. It has been reported incorporated carbon act as nucleation center for oxygen precipitation, therefore can cause in the lifetime degradation [6]. Moreover, there was a difference in the lifetime depending on the crystal growth conditions.

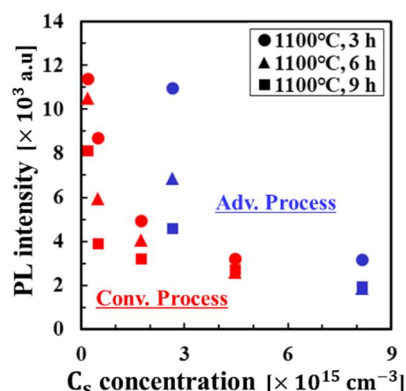


Fig. 1 Correlation between carbon concentration and PL intensity depending on crystal growth conditions.

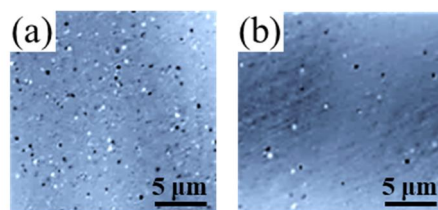


Fig. 2 IR-LST images after 1100°C for 6 h annealing. (a). Conv. process with carbon concentration of $1.7 \times 10^{15} \text{ cm}^{-3}$. (b). Adv. process with carbon concentration of $2.6 \times 10^{15} \text{ cm}^{-3}$.

We focus on the samples with similar carbon concentration under two different crystal growth conditions. Figure 2 shows the IR-LST images. Both the black and white dots observed in the IR-LST images are oxygen precipitates. It was

revealed that there was a clear difference in oxygen precipitation depending on crystal growth conditions, although the oxygen concentration and the carbon concentration are almost the same. It seems that the difference in oxygen precipitation occurred because the time to stay in the temperature region, in which precipitation nuclei are likely to be formed, differs depending on the crystal growth conditions.

Figure 3 shows the correlation between the total surface area of precipitates and the PL intensity as an index of the lifetime. Here, the shape of the precipitate was assumed to be spherical, and their total surface area was calculated from the measurement results of IR-LST. The interface between precipitates and Si matrix showed a good correlation with the lifetime [7]. This suggests that the interface is the dominant carrier recombination center. In addition, two types of crystal growth conditions showed different straight lines. Thus, it is assumed the recombination active defect density associated with the precipitate, possibly the dislocation density, is different depending on the crystal growth conditions.

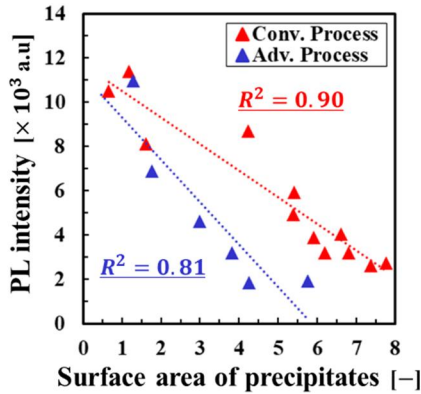


Fig. 3 Correlation between total surface area of precipitates and PL intensity depending on crystal growth conditions.

Figure 4 shows the optical microscope images after Sopori etching. In both processes, elliptical etch pits were observed. Elliptical etch pits were not observed before annealing process and the number of etch pits increased with increasing precipitate density. Those etch pits have been identified as dislocations caused by oxygen precipitates [3-5]. From Fig. 4, there was a clear difference in the shape of etch pits depending on the crystal growth conditions. From this, it is suggested that the propagation direction of dislocation differs between two samples [5]. It is considered that the difference in the propagation direction of dislocations is originated in the shape or size of the precipitates.

Figure 5 shows the correlation between carbon concentration and dislocation density evaluated by Sopori etching. As the carbon concentration increased, the dislocation density increased. Also, there was a clear difference in dislocation density depending on the crystal growth conditions. The difference in the dislocation properties accompanied with oxygen precipitation may be explained by the difference in the vacancy concentration depending on the crystal growth conditions. Rapid cooling may result in a high vacancy concentration and promote the strain relaxation caused by the oxygen

precipitation.

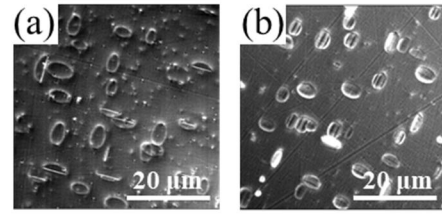


Fig. 4 Optical microscope images after 1100° C for 9 h annealing. (a) Conv. process with carbon concentration of $4.5 \times 10^{15} \text{ cm}^{-3}$. (b) Adv. process with carbon concentration of $8.2 \times 10^{15} \text{ cm}^{-3}$.

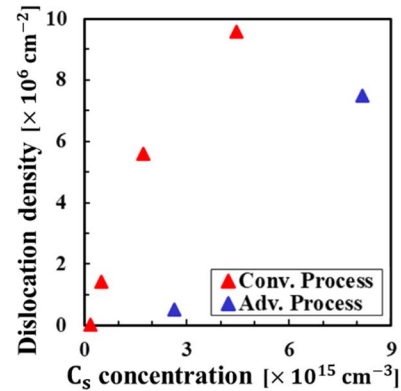


Fig. 5 Correlation between carbon concentration and dislocation density depending on crystal growth conditions after 1100° C for 9 h annealing.

4. Conclusions

We evaluated the effects of oxygen precipitation and dislocation formation depending on the crystal growth conditions on the minority carrier lifetime. Conclusions are as follows. Depending on the crystal growth conditions, there was a difference in the minority carrier lifetime and oxygen precipitation through annealing process. The interface at the oxygen precipitate/Si matrix was the dominant carrier recombination center. Depending on the crystal growth conditions, the dislocation density and propagation direction associated with oxygen precipitates were different. Therefore, it was revealed that oxygen precipitates and dislocations formation are controlled and lifetime deterioration is suppressed in Cz-Si which is kept at the high temperature and rapidly cooling during crystal growth.

Acknowledgements

Part of this work is supported by New Energy and Industrial Technology Development Organization (NEDO).

References

- [1] A. Borghesi *et al.*, J. Appl. Phys. **77**, 4169 (1995).
- [2] H. Bender *et al.*, Phys. Stat. Sol. A **86**, 245 (1984).
- [3] Y. Hamada *et al.*, J. Electrochem. Soc. **135**, 2606 (1988).
- [4] B. Sopori *et al.*, J. Electrochem. Soc. **135**, 2602 (1988).
- [5] B. Sopori *et al.*, Appl. Opt. **27**, 4678 (1988).
- [6] S. Zhang *et al.*, J. Cryst. Growth **411**, 63 (2015).
- [7] J. Murphy *et al.*, J. Appl. Phys. **118**, 215706 (2015).